RF BASED NAVIGATION FOR PRISMA AND OTHER FORMATION FLYING MISSIONS IN EARTH ORBIT

Michel Delpech, Pierre-Yves Guidotti, Sophie Djalal, Thomas Grelier, and Jon Harr
CNES, 18 avenue Edouard Belin, 31401 Toulouse Cedex.

ABSTRACT

A navigation system based on a new Radio Frequency sensor for relative positioning of satellites in formation has been developed for the PRISMA demonstration mission to be launched in 2010 in LEO. Navigation relies on an Extended Kalman Filter that includes an accurate modeling of relative dynamics and performs measurement biases estimation. Results obtained during the extensive ground validation show the satisfactory behavior of the filter in presence of measurement biases. The paper evokes how his function can still be applicable for future missions like Proba3 that fly on very elliptical orbits and what level of performances can be achieved.

1. INTRODUCTION

Radio Frequency (RF) metrology represents an appropriate technology for future rendezvous and formation flying missions that will fly beyond GPS access. It will be especially required to perform formation acquisition and guarantee collision avoidance whereas optical metrology will be used to achieve fine localization and positioning. Such a RF sensor derived from GPS receiver technology has been developed by TAS (Thales Alenia Space) under CNES & CDTI funding for the PRISMA technology mission to be in February 2010. This mission funded by the Swedish National Space Board involves two satellites flying on a Low Earth Orbit (LEO). It represents therefore a unique opportunity to validate this new RF metrology in representative conditions since the performance characterization on the ground suffers from numerous difficulties and limitations (high multi-path perturbations). CNES contributes by providing the RF sensor and Guidance, Control and Navigation (GNC) software in order to perform some Formation Flying experiments based on a technology that will be tested in space for the very first time.

A specific Navigation function has been designed to be used on top of this metrology and to work in close relationship with it, since it lacks the autonomy of usual sensors like star trackers. This function that provides assistance to the RF sensor will participate to the performance characterization activity. However, its main role consist in providing relative positioning data to the G&C algorithms during the closed loop experiments and the best possible performance was requested as a demonstration objective.

PRISMA is a “technology in-orbit testbed mission” [1] for demonstrating formation flying and rendezvous technologies, as well as flight testing of sensor and actuator technologies. The mission funded by the Swedish National Space Board (SNSB), is a multilateral project with contributions from CNES, DLR and DTU (Danish Technical University). The prime contractor is Swedish Space Corporation (SSC), responsible for design, integration and operation of the space and ground segments, as well as implementation of various in-orbit formation flying experiments. Launch is performed into a 700 km sun-synchronous orbit for an expected 10 months mission duration and all flight operations will be controlled via the Kiruna ground station.

The mission includes two spacecraft (a chaser and a target). The 140 kg chaser spacecraft (MANGO) has 3-axis reaction wheel based attitude control and 3-axis delta-V capability with 6x1N hydrazine thrusters. The 40 kg target spacecraft (TANGO) has no orbit control and its attitude control relies on coarse magnetic actuation.

Relative position is measured by 3 different sensors depending upon the experiment and the satellite distance: (1) Differential GPS system provided by DLR is the main relative positioning measurement system on PRISMA, and experiments will mainly be carried out for inter-satellite distances exceeding at least a few meters. (2) Visual based sensor (VBS) provided by DTU is based on a star tracker and will be used from long distances (to detect the target up to several hundreds of kilometers) down to several meters where the Target pose will be extracted – (3) RF metrology subsystem (FFRF) provided by CNES will be used for inter-satellite distances from 3 m to 30 km.

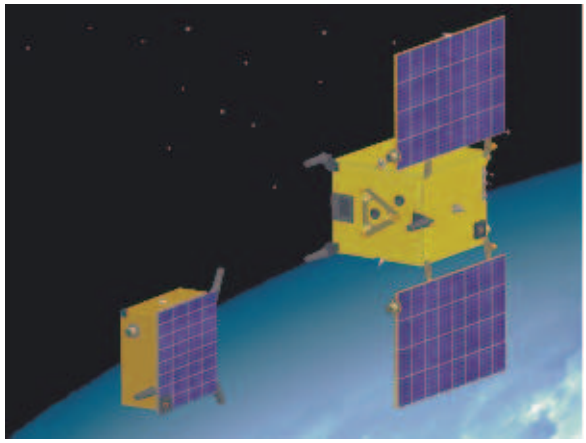

Figure 1 MANGO (right) and TANGO (left) PRISMA spacecraft

CNES participates to this mission through the FFIORD experiment [2] (which name stands for Formation Flying In-Orbit Ranging Demonstration). The main objectives of this demonstration are twofold: (1) Perform a flight validation of FFRF subsystem, (2) Test the different on-board algorithms necessary to autonomously maintain 2 satellites in close formation using data from FFRF sub-system.

The FFIORD experiment involves therefore two main contributions: the RF metrology and a software module that is integrated directly into the MANGO on board software. This additional software allows CNES to take over spacecraft control and run various FF activities in a dedicated GNC mode: proximity operations with tight control, loose station-keeping, rendezvous, collision avoidance. These FF activities that involve different guidance algorithms rely on FFRF data which is processed by a common Navigation functionality.

This paper will present the RF sensor specific features (architecture, functional and performance limitations). Next, it will detail the design of the Navigation function essentially from the algorithm point of view. The validation approach will be described later with a presentation of the main performance features. The last part will discuss how this Navigation function that was optimized for the LEO context can be still reused for future missions flying in high elliptical orbits like Proba3 and what level of performances can be achieved.

2. FFRF SENSOR

2.1 General purpose

The FFRF Sub-System [3] is designed to offer relative positioning for up to 4 satellites flying in formation. It can produce for each spacecraft relative position, velocity and Line Of Sight (LOS) measurements concerning all its companions. The accuracy level is sufficient for a first metrology stage devoted to formation acquisition and coarse station-keeping. If higher accuracy is needed, subsequent optical metrology sub-systems shall take over.

The subsystem is constituted of one FFRF terminal and up to 3 sets of antennas on each satellite of the constellation. A set of antennas can be either a triplet (1 Rx/Tx master and 2 Rx slaves) or a single Rx/Tx antenna. The terminal operates by dual frequency in S-band, and each terminal transmits and receives signals to and from all the other satellites of the constellation in a TDMA based pattern. Ranging and angular measurements are extracted from received signals and are used for computing relative position, velocity and line-of-sight. In addition to providing relative navigation measurements, the FFRF subsystem also provides an inter satellite link (ISL) as auxiliary functionality (up to 12 kbps).

The FFRF subsystem is specified to provide the following information every second:

- Inter-satellite distance (specified accuracy = 1 cm)
- Azimuth and elevation of line-of-sight between two satellites (specified accuracy < 1°)
- Time bias between the two satellite clocks

2.2 Measurement principle

The measurement approach is inspired by the GPS system. Using multi-antenna bases (triplets) and TDMA sequencing, each terminal transmits and receives a GPS C/A navigation signal modulated on two S-band carrier frequencies (L1 and L2). Since every terminal can be equipped with both transmitter and receiver, each satellite is then able to make ranging and LOS measurements with every other satellite. First, coarse measurements are made using the ranging from the C/A code, and then fine measurements with centimeter accuracy are performed using carrier phase measurements. The dual frequency allows the system to perform carrier ambiguity resolution using a wide lane, while 2-way measurements are used to account for the relative clock drift of the platforms. LOS measurements are made by measuring the carrier phase difference between the master and slave antenna on the triplet antenna base. Attitude, though, has to come from an external attitude sensor such as a star tracker.

Three types of raw data are coming from Rx/Tx antennas: (1) pseudo-code measurement, (2) phase measurement on L1 carrier, (3) phase measurement on wide-lane obtained by combination of L1 and L2 carriers. The raw data coming from Rx only antennas are two-fold: (1) delta phase measurement on wide-lane, (2) delta phase measurement on S1 carrier.

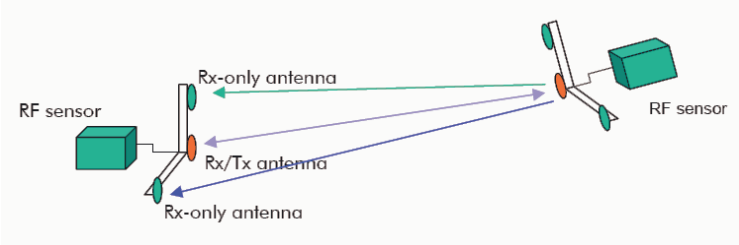

Figure 2. Two-satellite FFRF S/S configuration

For PRISMA, the configuration is not symmetrical and TANGO satellite is equipped with three Rx/Tx antennas on different faces to ensure full space coverage (Figure 2), without any Rx only antenna. MANGO satellite is the only one equipped with a full antenna triplet (1 Rx/Tx and 2 Rx) that is required to determine the full precise positioning (both distance and LOS) of the companion satellite.

2.3 Integer ambiguity resolution

Carrier phase, used for LOS angles and distance computation, is measured modulus 2π. This means that an integer number of cycles remains unknown and must be solved during initialization to reach

nominal precision. After signal acquisition, the initialization procedure includes therefore an Integer Ambiguity Resolution (IAR) function that implies the filtering of the different available signals to improve knowledge in a stepwise process.

Because of the potential presence of significant biases due to multi-path effects that are direction dependent, the procedure always starts by removing the ambiguity on the Line of Sight. When the LOS is determined with the highest accuracy available from L1 carrier measurements, it becomes possible to apply a multi-path cartography and then reach a higher precision on the distance estimation. By filtering the wide-lane data over time, the distance ambiguity on distance can be removed to achieve the final precision (centimetric).

In the current design, the FFRF sensor cannot remove by itself the ambiguity on the Line of Sight since the precision achievable with the wide-lane is larger than the L1 carrier wavelength (13 cm). To solve the problem, the spacecraft is rotated along the axis normal to the base of antennas. By a combined processing of the FFRF signals and the satellite attitude information, the ambiguity can be removed after a rotation of about 50°.

Note that the instrument sensitivity to multi-path effects requires therefore their mitigation through a calibration procedure in anechoic chamber. This procedure performed with representative allows to elaborate multi-path correction tables in function of LOS angles that are stored in sensor memory and used during the flight. Residual biases will however remain in space and the ability to estimate them is therefore an important means to improve final performances.

2.4 Cooperation with the GNC system

The FFRF sensor is capable to deliver two types of metrology information at 1 Hz rate:

(1) RF signal raw data composed of pseudo-code, phase, delta-phase measurements from each terminal along with clock bias between terminals,

(2) Position, Velocity and Time (PVT) for the companion satellite: this data represents a single snapshot that is obtained using basic geometric relations after removal of the signal ambiguities.

Two options can be therefore envisioned to implement a RF based Navigation function in the GNC system: either rely on the raw data as input and implement the higher metrology functionalities (signal filtering, IAR) along with the state estimation filter, or use the already processed PVT as data input. The first option consists in removing all smartness from the sensor and use it only as a RF signal acquisition unit. It allows an integrated design with full functional visibility and algorithm tuning capability but it increases of course the computational load of the spacecraft OBC. The second option which keeps the higher metrology functions within the sensor has been selected for the PRISMA mission in order to reduce the technical and planning risks. This architecture implies however that the GNC system provides some assistance to the FFRF sensor to cope with its reduced autonomy. This assistance briefly described here-below is twofold:

1. Assistance for IAR: During initialization, TANGO and MANGO attitude are provided to solve the LoS ambiguity. This data is transmitted during the rotation maneuver.
2. Assistance for signal acquisition and navigation: This assistance is provided optionally to speed up the acquisition of the RF signal at sensor power-up or after tracking loss, and to help the PVT process to get running after some temporary loss of data. For that purpose, aiding data is provided with Figures Of Merit (FOM) values so that the sensor can determine whether the IAR process needs to be performed again or not. This data is also used to detect cycle slips (if the displacement exceeds half the wavelength in one period) and correct the measurement accordingly if no doubt remains.

3. RF BASED NAVIGATION FUNCTION

3.1 Problem description

The RF Navigation Function constitutes the core element of the CNES GNC system implemented on MANGO satellite. This function is active whenever the FFRF sensor is running. Initially, it is used in open loop for sensor characterization and later in closed loop during the FF experiments. It provides MANGO relative state with respect to the companion spacecraft (TANGO) which is then used by guidance and control algorithms. In addition, it performs also FFRF sensor management which involves computing aiding data and above all monitoring (sensor re-initialization can be actually triggered automatically in some anomaly situations).

The objective is to implement a Relative Navigation function for two satellites flying on any type of planetary orbit (high eccentricity included) and relying on possibly biased relative measurements. Note that PRISMA orbit eccentricity is quasi-circular (e = 4e-3) and allows to make model simplifications. However, navigation design has been performed in the more general case to enable a better applicability to future missions flying in Earth orbit.

Using measurements provided by the FFRF sensor, the problem consists in determining with the best possible accuracy the position and velocity of MANGO satellite centre of mass expressed in the companion Spacecraft Local Orbital frame (later referred as SLO). SLO frame is defined as follows: Z_{SLO} axis is directed to Earth centre, Y_{SLO} axis is opposed to the orbital angular momentum vector and Z_{SLO} complete the orthonormal frame.

An important feature to be included in the design is the capability to estimate the angle biases that affect FFRF measurements mostly due to multipath effects. If not mitigated, the LOS biases will particularly impair the performances at long range since lateral errors are proportional to distance (1 degree bias produces lateral errors of 17 meters at 1 km range).

Measurement equation

The FFRF sensor measurement vector at date k (z_k) is described here-after:

$$z_k = [x_{LOS}, y_{LOS}, d]^t \quad (1)$$

$$d = (x_{RF}{}^2 + y_{RF}{}^2 + z_{RF}{}^2)^{1/2} + b_d + \eta_d \quad (2)$$

$$x_{LOS} = x_{RF}/d + b_X + \eta_X \quad (3)$$

$$y_{LOS} = y_{RF}/d + b_Y + \eta_Y \quad (4)$$

where (x_{RF}, y_{RF}, z_{RF}) are the coordinates of the TANGO S/C Rx/Tx antenna in the MANGO RF terminal reference frame (the origin is located at the phase centre of the Rx/Tx antenna, z axis is pointed along the antenna axis whereas x and y are defined arbitrarily to get an orthonormal frame).

(b_d, b_X and b_Y) represent the cumulated bias affecting respectively the distance, Xlos and Ylos measurements whereas (η_d, η_X, η_Y) represent the corresponding noise vector. The biases affecting LoS angles are due to residual electrical biases along antenna RF cables, uncertainty on the location of Rx antennas centre of phase and residual multi-path errors. Distance and LoS noise components are non correlated since they are performed at different time intervals. They are modelled as Gaussian random variables with zero mean.

If we relate FFRF measurements to the components of the state vector (position only), the expression involves both spacecraft attitude: MANGO attitude for the most part and TANGO to a lesser extent through the lever arm between the c.o.g. and the antenna. Since spacecraft attitudes are provided in inertial frame, the relation involves also the attitude of SLO frame.

The measurement equation can be finally summarized by the following non linear equation:

$$z_k = h(y_k, q_{SLO}, q_M, q_T) \quad (5)$$

where y_k is the filter state vector and q_{SLO}, q_M, q_T are respectively the attitudes of the SLO, MANGO and TANGO frames.

An Extended Kalman Filter formulation is therefore required before considering the model for state evolution.

Relative dynamics model:

To maximize navigation performances, the navigation filter must include a dynamic model of the relative motion. Several formulations have been considered for the FFIORD implementation:

- ⇨ Clohessy-Wilshire [4] (CW) equations represent a valid option for circular or very low eccentricity orbits since they are time invariant and enable to compute a state transition matrix.
- ⇨ Yamanaka-Ankersen [5] (YK) equations take into account orbit eccentricity and can be integrated analytically to produce a state transition matrix. The computational load is significantly heavier with respect to CW transition matrix and its expression is position dependent. The formulation does not include differential acceleration due to J2 and higher gravity terms.
- ⇨ Tschauner-Hempel equations [6] have been developed to model the satellite relative motion on Non Keplerian orbits and include the differential acceleration due to J2. No closed form solution for the state transition matrix can be obtained from these equations and it is therefore required to integrate them numerically. Given their computational complexity, an alternate approach consists in computing the relative state by difference of the two satellites absolute states which are obtained by orbital propagation. The principle is to implement a propagator based on a simplified but computationally efficient dynamics model.

These different options have been actually implemented in the Navigation function and can be selected via TC. Additional options to consider concern the computation of the SLO frame attitude that is derived from TANGO predicted / estimated position. Several sources are available on PRISMA: data from TLE propagator (SGP4) implemented by SSC, data from GPS navigation provided by DLR. Another possible solution is also the output of the simplified absolute dynamics model implemented for FFRF navigation. The latter one has been chosen for FFIORD along with GPS navigation solution. Table 1 summarizes the different configurations that can be triggered for the FFRF navigator.

Local Orbital frame attitude	Relative dynamics model	Id
Target position (GPS data)	Clohessy-Wilshire equations	1
	Yamanaka-Ankersen equations	2
	Difference of absolute states obtained by numerical integration	3
Target position obtained from simplified absolute propagator	Clohessy-Wilshire equations	4
	Yamanaka-Ankersen equations	5
	Difference of absolute states obtained by numerical integration	6

Table 1: RF Navigation configurations

3.2 Algorithm description

The algorithm is detailed here-after for the option based on the difference of absolute states (3 or 6). In that case, the computation of the relative state can be summarized as follows:

$$\hat{x}_{k+1}^{T} = g(\hat{x}_{k}^{T}, \tau) \quad (6)$$

$$\hat{x}_{k+1}^{M} = g(\hat{x}_{k}^{M}, a_{k}^{M}, \tau) \quad (7)$$

$$\hat{y}_{k+1} = T_{ECI->SLO}.(\hat{x}_{k+1}^{M} - \hat{x}_{k+1}^{T}) \quad (8)$$

The function *g( )* represents the integration of a dynamic model equation that includes J_0 and J_2 gravity terms as well as drag acceleration. The equation is integrated numerically using a 4th order Runge-Kutta method.

$\hat{x}_k^T$ and $\hat{x}_k^M$ represent the predicted absolute state of respectively TANGO and MANGO spacecraft at iteration k whereas a_k^M is the external acceleration applied to MANGO and measured with accelerometers.

τ is the integration period (1 second).

The transform $T_{ECI->SLO}$ converts the relative position-velocity vector (6 components) expressed in Earth Centered Inertial frame (ECI) into SLO frame.

This relative state in SLO frame is updated using the true FFRF measurements, the expected measurements and the Kalman gain according to relation (11)

$$\tilde{y}_{k+1} = \hat{y}_{k+1} + f(z_{k+1} - h(\hat{y}_{k+1})) \quad (9)$$

$$\tilde{x}_{k+1}^{M} = \tilde{x}_{k+1}^{T} + T_{ECI->SLO}^{-1}(\tilde{y}_{k+1}) \quad (10)$$

The Navigation function includes therefore the computation of the SLO frame attitude since it propagates the orbital position of TANGO spacecraft. The accuracy of this predicted state tends however to decrease over time due to the use of a simplified model. The scheme that was adopted to limit the drift was to update TANGO absolute state on a regular basis (every day) via telecommands.

Bias estimation:

FFRF measurement are not the only sources of bias in the measurement equation. We need to consider also MANGO S/C attitude biases due to star tracker misalignment (alignment uncertainty is 0.34 deg at 1 sigma) that will bring another bias angle contribution. However, the presence of axes coupling in the measurement equation and the dynamic model offers the capability to estimate the overall direction angle biases (i.e. the sum of all contributing terms). For that purpose, EKF state vector includes 8 components: 3 position (x, y, z) and 3 velocity coordinates (v_x, v_y, v_z) in SLO frame as defined previously plus two exogeneous states corresponding to the direction angle biases (b_{xlos}, b_{ylos}). However, it is important to state that the algorithm assumes the presence of constant biases which implies that TANGO LoS is maintained quasi-constant through a specific attitude guidance (TANGO pointing).

Besides, this bias estimation capability can be turned off if needed and in that case the filter state dimension is reduced to 6.

Covariance evolution and state update

Kalman gain needs to be updated periodically since it is configuration dependent and this imposes to update the state covariance matrix as well. Here, the propagation of this covariance matrix represents a tough problem if the accurate model used for state prediction is to be considered. For

computational efficiency, we need to rely instead on a sub optimal model which provides a state transition matrix. YK and CW transition matrices are therefore chosen as filter options and they are both implemented and made selectable by the user via a configuration parameter.

Propagation of the state covariance P relies on an 8x8 state transition matrix deduced from CW or YK equations (in presence of eccentricity) and a 2x2 identity matrix to propagate the bias states.

$$\hat{P}_{k+1} = F.\tilde{P}_k.F^t + Q \tag{11}$$

$$F = \begin{bmatrix} F_{6x6} & 0 \\ 0 & I_{2x2} \end{bmatrix} \tag{12}$$

Q is a 8x8 state noise covariance matrix with only diagonal terms. The non correlation between distance and LoS vector measurements allows to update the filter state separately and reduce the computational cost.

$$K_k^d = \hat{P}_k.(H_k^d)^t.(H_k^d.\hat{P}_k.(H_k^d)^t + R_k^d)^{-1} \tag{13}$$

$$\tilde{P}_k^1 = \hat{P}_k - K_k^d.H_k^d.\hat{P}_k \tag{14}$$

$$\tilde{y}_k^d = \hat{y}_k + K_k^d.(z_k^d - h_d(\hat{y}_k)) \tag{15}$$

$$K_k^{LoS} = \tilde{P}_k^1.(H_k^{LoS})^t.(H_k^{LoS}.\tilde{P}_k^1.(H_k^{LoS})^t + R_k^{LoS})^{-1} \tag{16}$$

$$\tilde{P}_k^1 = \tilde{P}_k^1 - .K_k^{LoS}.H_k^{LoS}.\tilde{P}_k^1 \tag{17}$$

$$\tilde{y}_k = \tilde{y}_k^d + K_k^{LoS}.(z_k^{LoS} - h_{LoS}(\tilde{y}_k^d)) \tag{18}$$

K_k^d and K_k^{LoS} represent the Kalman gains associated to distance and LoS whereas H_k^d and H_k^{LoS} correspond respectively to the linearization of the distance and LoS measurement equation defined in (5).

$\hat{y}_k$, $\tilde{y}_k^d$ and $\tilde{y}_k$ are respectively the predicted state for iteration k, the updated state with the distance measurement and finally the updated state taking into account both measurements.

R_k^{LoS} and R_k^d represent respectively LoS (2x2) and distance (1x1) measurement noise covariance matrices.

Measurement synchronization

The formulation presented here-above assumes that all filter inputs are synchronous, and delivered without any latency. This is actually true for PRISMA system data (attitude quaternions and rates, applied acceleration measurements) which are synchronized before delivery. This is not the case however for FFRF measurements which are time stamped by the sensor internal clock. These data are subject to some latency induced by PRISMA data handling system and the sensor itself (the distance measurement implies the processing of pseudo-ranges from terminals on MANGO and TANGO and it may arrive up to 3 seconds after the LoS measurement).

In order to compute the innovation due to distance measurement, the filter determines first the expected measurement at date $t_d = t_{LoS} - \tau$ using the current distance d, distance rate $\dot{d}$ and external acceleration a projected along the distance vector:

$$\hat{d}(t_{LoS} - \tau) = \hat{d}(t_{LoS}) - \dot{d}(t_{LoS}).\tau - \frac{1}{2}a(t_{LoS} - \tau, t_{LoS}).\tau^2 \tag{19}$$

The innovation due to distance is then obtained by applying the Kalman gain defined previously in equation (21).

$$u^d(t_{LoS}-\tau) = K^d_{t_{LOS}}.(d(t_{LoS}-\tau) - \hat{d}(t_{LoS}-\tau) \quad (20)$$

Next it can be propagated to the date of LoS measurement using either CW or YK state transition matrix:

$$u^d(t_{LoS}) = \phi(t_{LoS}-\tau, t_{LoS}).u^d(t_{LoS}-\tau) \quad (21)$$

The external acceleration due to thrust is not to be taken into account in relation (21) since it is already considered in the prediction equation (7).

Covariance update in presence of maneuvers

State propagation benefits from the knowledge of satellite accelerations during thrust which is provided by accelerometers on MANGO spacecraft. The measurement error amplitude is however high enough to affect negatively estimation performances. A possible approach consists in increasing the values of the state noise covariance matrix by an additional and constant term of uncertainty corresponding to the mean contribution. The effect of maneuvres is thus minimized but performances are reduced during the free flying intervals. The alternative approach that has been selected consists in introducing an additional term only during maneuvers application.

$$Q_v^i = Q_v^i + C^i.(a_m^i)^2 \quad (22)$$

a_m^i represent the applied thrust and C^i is a coefficient of uncertainty.

Note that the maximum acceleration is 7 mm/s² (1 N thrust on a 140 kg spacecraft) and the uncertainty being considered is in the [1-2] mm/s² range.

3.3 Filter initialization / sensor management

The Navigation filter can be initialized before FFRF sensor is powered and delivers measurement data. Upon activation, the filter starts the orbit propagator using data uploaded by telecommand (TANGO absolute position and associated GPS time stamp) and waits for the sensor to be alive. No relative state will be actually computed by the filter until the IAR process for Line of Sight is not achieved. When this process is over, Navigation start processing data. Distance measurement can be valid either from code, wide-lane or carrier depending on how long the Navigation is configured to wait (the whole process of noise filtering can take up to 1000 s to achieve the targeted 1 cm accuracy).

The initial relative position is then directly computed from this data set using the inverse of the measurement equation (5). Relative velocity is then obtained through the processing of several samples. In a cold start configuration, the initial state accuracy may be quite coarse if TANGO Line of Sight is beyond a 30° half cone around the antennas axis because of the larger bias expected from multi-path. For better performances, it is planned to reorient MANGO spacecraft to get into a LOS area less perturbed by multi-path (and maintain TANGO pointing).

The navigation filter is designed to reject FFRF measurements when the difference between the expected and the true values exceed a given threshold specified by TC. If the measurements are not available or declared invalid, the filter propagates relative data over a specified time horizon and resets the FFRF sensor when the time-out is reached.

The Navigation filter includes also some internal reset capability in case of major problem like a divergence of the state covariance matrix which is detected by monitoring its values against some given min and max bounds. However this situation is not critical in the PRISMA context and will

not imply contingency actions since differential GPS data is always available and allows to recover a proper relative state if needed.

4. VALIDATION RESULTS

4.1 Validation approach

The Navigation function alone and integrated with the other GNC algorithms that compose the CNES software have undergone extensive tests that were performed in two main successive steps:

1. the first step performed at CNES consisted in simulation campaigns run on two dedicated tools: a MATLAB/Simulink simulator and an hybrid simulator allowing to run the auto-coded software on a representative environment (same LEON3 processor and Real Time Operating System)
2. the second step has been performed at SSC premises first on the avionics test-bench and finally on the real satellites with emulators or stimulated equipment.

Most of the validation work has been performed in the Simulink environment with progressive improvement in the sensors and actuators modeling but also the introduction of representative data latencies and various time references. In particular, a numeric simulator representing the accurate behavior of the FFRF sensor has been developed: it includes a RF signal generator as well as the real PVT software running in the sensor. Monte Carlo simulations have been run to assess the navigation robustness to various parameter variations including FFRF sensor peculiar behavior and also to perform the most appropriate filter tuning.

In the sequel, we illustrate the performances of the navigation from the following points of view: (1) the ability to estimate measurement biases, (2) the benefit of taking into account J2 term in the relative dynamics model. The behavior is finally shown for a real experimental scenario (rendezvous from 10 km distance) that has been run several times in SSC test bench.

4.2 Bias estimation

The test scenario which involves filter initialization at start consists in performing state estimation over two orbits (12000 seconds duration) in a quasi static relative configuration. For this experiment, MANGO is maintained pointed to its companion spacecraft so that the residual multi-path error (not corrected by calibration) will be constant and will add-up to the other LoS measurement biases. The test is performed at various distances (20 times at each location) and the estimation factors of merit are represented by the error mean and standard deviation over the last orbit (6000 seconds). Measurement bias is 1° for both LOS components which correspond to a 17 meters lateral error for every kilometer of spacecraft separation (150 m at 9 km range).

Filter tuning is performed via the state noise covariance matrix parameters (8 diagonal terms). The selected tuning assumes an acceleration noise of 1 µm/s² on the X,Y and Z axes. Identical figures are taken concerning the noise affecting the bias states to be estimated.

Q = diag ([0, 0, 0, 1e-12, 1e-12, 1e-12, 1e-12, 1e-12])

Measurement noise values (3 sigma) are respectively 0.6° and 0.09° for X and Y LOS angles and 5 mm on distance.

Figure 3.1 show the performances obtained for distances for the following set of distances [30, 100, 300, 1000, 3000, 6000, 9000 m]. Blue and red stars correspond respectively to mean error and variance. First line represents along track estimation error (in meters) whereas second and third lines yield the cross track and radial errors expressed in LoS angles (radians). Horizontal axis displays the distance case id (1 = 30 m, 2 = 100 m, …7 = 9000 m). Figure 3.1 and 3.2 show the benefit of bias estimation error that provides a performance improvement ratio of about 100 on along track and radial errors.

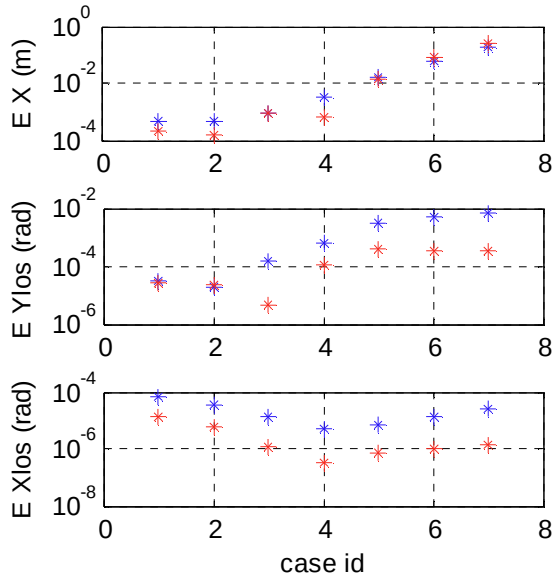

Figure 3.1 Bias estimation active

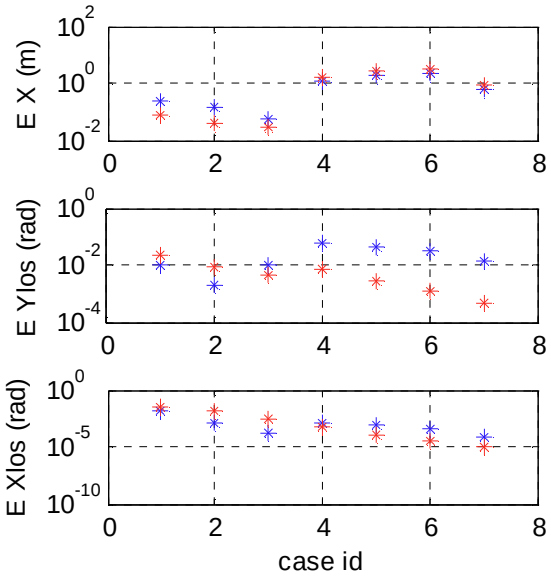

Figure 3.2 Bias estimation inactive

We notice some performance degradation that is function of distance as expected but it is particularly significant on Y axis (off-track) where the sensitivity to initial errors is increased due to the absence of dynamic coupling with other axes. This effect is illustrated with simulation plots for two cases at different distances (d =1 km and d = 9 km).

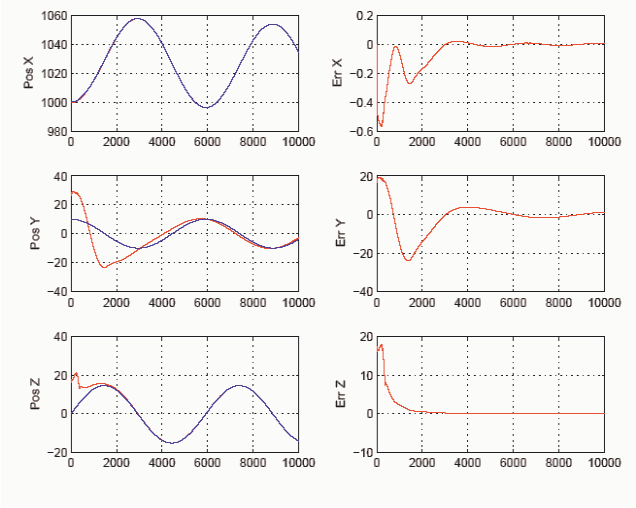

Figure 4.1 Navigation performances at distance = 1 km

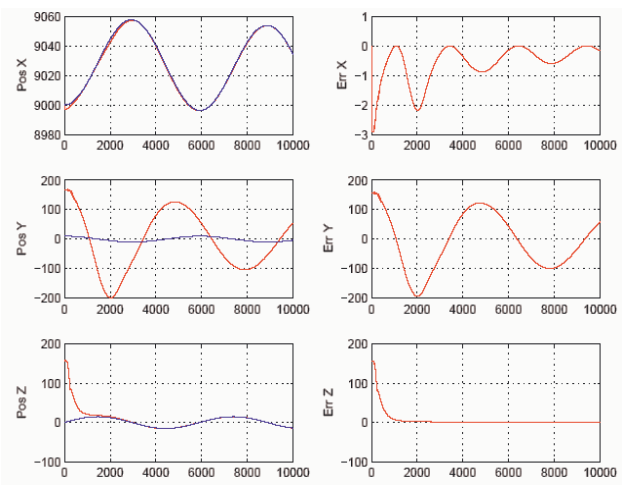

Figure 4.2 Navigation performances at distance = 9 km

Figure 4.1 shows the excellent behaviour of the filter that cancels the bias in a few thousands seconds (convergence is significantly faster on Z axis due to the in plane axes coupling). This allows getting performances in the centimetre range on both radial (Z) and cross-track axes (Y).

A degradation of cross-track performances (Y axis) at long range is illustrated on Figure 4.2: the settling time gets much longer and filter oscillations are still around a 100 meters after 8000 s. This shows on this axis the sensitivity of the filter to large initial errors (150 m). The behaviour remains however excellent in the plane since the error reaches quickly the centimetre level.

To summarize, he benefit of bias estimation is unquestionable since the in plane relative motion can be determined for all ranges with high accuracy. The capability to estimate accurately the crosstrack

bias is degraded when distance increases but this limitation has no impact on the formation acquisition performances that rely mostly on the in plane motion knowledge (see later §4.4).

4.3 Influence of J2 term

The benefit of taking into account J2 term in the relative dynamics model has been assessed for state estimation at short and medium range (distances considered: 30 m, 100 m, 300 m 1000 m). Tests are performed with two configurations: the first one including J2 term (difference of absolute states obtained by numerical integration) and the other without (Yamanaka-Ankersen model). Performances are again expressed as mean and variance error over the whole 2nd orbit after navigation start. They are shown on bar graphs (mean: blue, variance: red) related to the four distance cases.

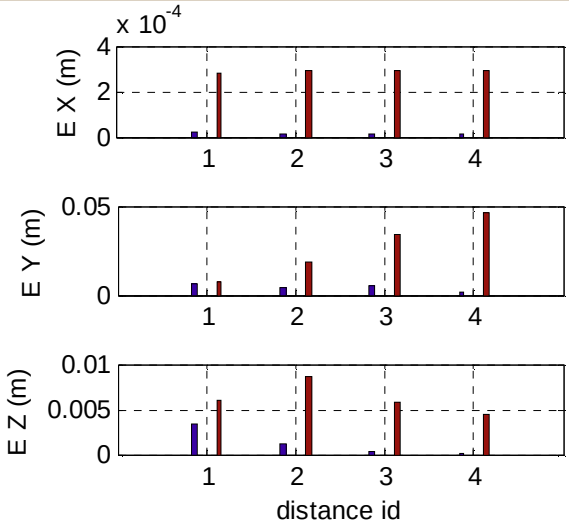

Figure 5.1 Performances taking into account J2

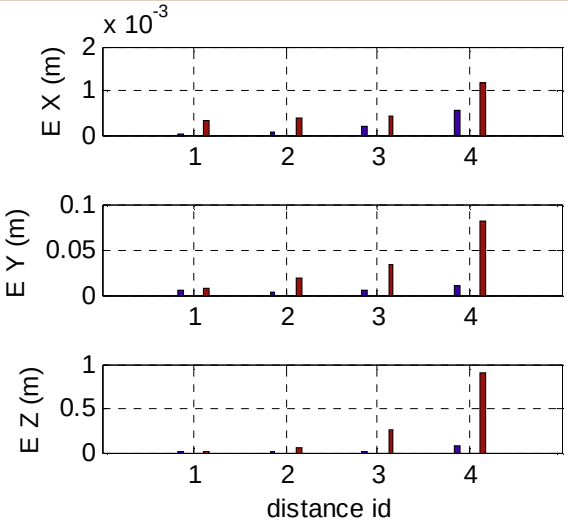

Figure 5.2 Performances taking into account J2

As expected, the main difference is observed on Z axis and the estimation error at 1000 m range reaches almost two meters when the J2 term is not included (the error is below 1 centimeter in the other case). This error will increase of course if the satellites separate further. It is still quite observable at shorter distances (100 m) as it is shown on Figure 6.1 and 6.2.

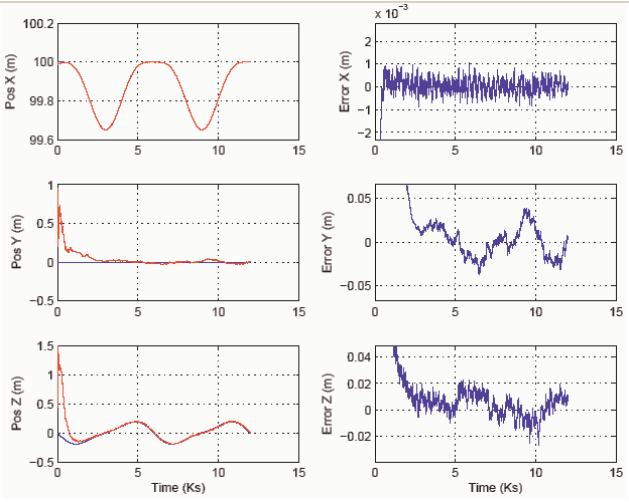

Figure 6.1 Performances taking into account J2

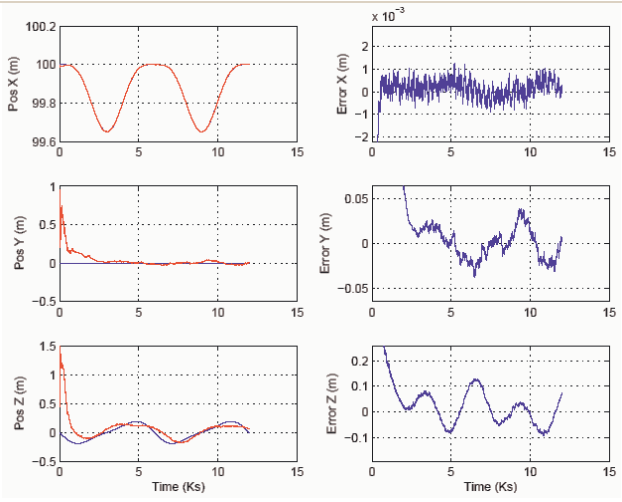

Figure 6.2 Performances taking into account J2

4.4 Illustration of navigation performances during a rendezvous experiment

The test scenario corresponds to a type of experiment that will be performed during the mission. It is initiated at 10 km distance and after a drifting period of about one orbit for navigation convergence a rendezvous is started to drive MANGO to the relative location [100, 0, 0] over 11 orbits. Next, the satellite is maintained tightly in this location for 10000 s and finally is injected into a relative orbit-keeping with 30 m radial and 30 m off-track components.

The simulation that spans a large range spectrum offers a complementary illustration of navigation performances in presence of bias (1° on LoS) and manoeuvres. The left plot column shows the real relative position (blue) superimposed with the estimated one (red). Right column presents the estimation error on the 3 SLO axes (along track, cross-track and radial).

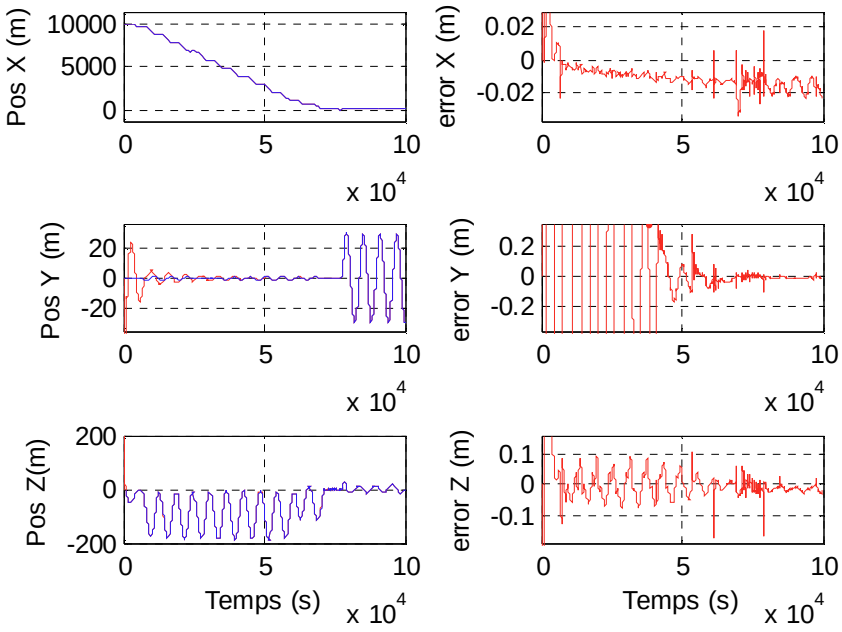

Figure 7. Navigation performances during a 100000 s rendezvous scenario

As expected, the cancellation of the 175 m initial radial error is quite fast (below 1 m in 2000 s) whereas it takes about ½ day to get to that level on the cross-track component and mainly because the distance gets smaller. It is interesting to note that the rendezvous accuracy is not affected by the cross-track knowledge error (less than 20 cm lateral error on the destination point).

5. APPLICABILITY TO FUTURE MISSIONS

Even though Lagrangian points constitute a very attractive area to place satellite formations due to the very quiet gravity environment, several missions have been envisioned to be flown in Earth high elliptical orbit. Simbol-X bi-satellite mission cancelled this year was designed to fly along a 4 day period orbit (20000 – 200000 km). Similarly, the PROBA-3 [7] formation flying demonstration to be launched in 2013 involves two satellites on a 24 h high elliptical orbit (800 km – 71200 km). For these missions, the FFRF sensor has been regarded as the baseline sensor to perform formation acquisition and take over control in contingency situations. It is therefore interesting to investigate whether bias estimation can still bring some benefit on such a different orbital environment.

First of all, the navigation functionality developed for PRISMA can be used with no significant change since the relative model takes into account orbit eccentricity. Due to the high eccentricity (e = 0.83), the evolution of the state covariance matrix relies now on the Yamanaka Ankersen state

transition matrix. To reduce the computational load, the matrix is only updated when the satellite anomaly change exceed a given threshold (1°).

A test scenario has been defined to illustrate the applicability of the PRISMA Navigation function. This scenario consists in performing state estimation over a complete 24 hours orbit with an initial configuration at apogee (assuming the two satellites are released at this location from a single carrier and separated by 1 km). The two satellites are flying on the very same orbit with a certain separation and continuous visibility is assumed. LoS measurement bias is identical as before (1°).

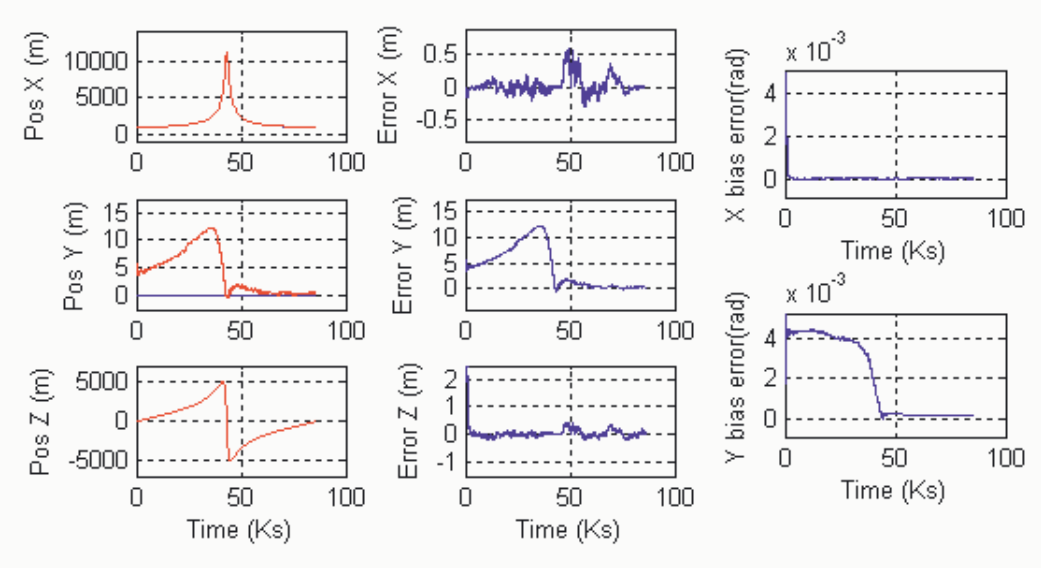

Figure 8. Navigation performances on a High Elliptical Orbit

Figure 8 show that in plane performances are remarkably good with a quick convergence of the corresponding bias estimator (Xlos bias). On the contrary, we observe poor out of plane performances on most of the orbital arc starting from apogee since the spacecraft is in quasi free-flying conditions. The situation improves however during the perigee passage when the relative distance varies quickly and provides therefore some strong coupling with Y axis. This allows the bias estimator to get rapidly close to the desired value. As expected, the bias estimator gets quasi-stationary again during the cruise to apogee.

These results are very preliminary and need to be consolidated through more extensive simulations. They indicate however that bias estimation can be envisioned even though the mean orbital motion is much lower than in LEO.

7. CONCLUSION

A Navigation function based on a new RF metrology system has been developed in the frame of the PRISMA technology mission to be flown beginning of 2010. This function estimates the relative state of one spacecraft with respect to its companion as well as two angular measurement biases. It implements an Extended Kalman Filter including several relative dynamic models. The most accurate computes the relative state by difference of the two satellite absolute states provided by two independent and simplified orbit propagators. This formulation allows taking into account orbit eccentricity and higer gravity term such as J2. This Navigation function has been exhaustively tested on various simulators including test benches with sensors in the loop and the results are very promising from the performance and robustness point of view. Bias measurement has shown particularly its benefit in the LEO environment by its capability to improve performances at long range. The applicability of the Navigation function including the bias estimation capability has been also identified for high elliptical orbit through a preliminary analysis.

REFERENCES

[1] S.Persson & al, Prisma-An Autonomous Formation Flying Mission, Small Satellite System and Services Symposium, 25-29 Sept.2006, Chia Laguna, Sardinia, Italy.

[2] J.B.Thevenet and al., A Generic Radio-Frequency Subsystem For High Altitude Formation Flying Missions, 3rd International Symposium on Formation Flying Missions and Technologies, Noordwijk, The Netherlands, 23-25 April 2008.

[3] J.Harr & al; The FFIORD experiment. CNES RF metrology validation and formation flying demonstration on PRISMA, 3rd International Symposium on Formation Flying Missions and Technologies, Noordwijk, The Netherlands, 23-25 April 2008.

[4] W.Clohessy and R.Wiltshire, Terminal Guidance System for Satellite Rendezvous,Journal of the Aerospace Sciences, Vol.27, No.9,1960, pp.653-658

[5] Yamanaka-Ankersen; New state Transition Matrix for Relative Motion on an Arbitrary Elliptical Orbit; Journal of Guidance, Control and Dynamics, vol 25, n°1, 2002, p60-66

[6] J.Tschauner and P.Hempel, Rendezvous with a Target in an Elliptical Orbit, AIAA Journal, Vol.8, 1970

[7] L.Tarabini & al., PROBA-3 Formation flying Guidance Navigation and Control, 3rd International Symposium on Formation Flying Missions and Technologies, Noordwijk, The Netherlands, 23-25 April 2008.

◄ BACK TO SESSION DETAILED CONTENTS ◄ BACK TO HIGHER LEVEL CONTENTS